Lateral Resistance of Hybrid Monopile-Footing Foundation in Cohesive Soil for Offshore Wind Turbines

Lei Huang*, Jiangtao Yi, Bangju Liu, and Xiuzhe Wang

School of Civil Engineering, Chongqing University, Chongqing 400045, China;
Email: LeiHuang@cqu.edu.cn (L.H.)

***Abstract*—Hybrid monopile-footing foundation, i.e., the addition of circular load-bearing plates at the mudline of large diameter offshore piles subjected to large horizontal-moment loads, is an innovative offshore structure. In this paper, the ultimate horizontal bearing capacity of hybrid monopile foundations is investigated by numerical simulation, in ABAQUS v6.14-1, using the small strain finite element method to simulate hybrid monopile-footing foundation subjected to lateral loads and to study the horizontal bearing performance of hybrid monopile-footing foundations in saturated soft clay soils with different circular footing foundation diameters. The Tresca model is used in this simulation and the validity of this simulation is verified by comparing the analysis with the theoretical and numerical solutions of circular footing foundations. The lateral load bearing performance of hybrid monopile foundations in soft clay soils is obtained by comparing and analysing the ultimate lateral bearing capacity for different circular footing foundation diameters.**

***Keywords*—hybrid monopile-footing foundation, undrained capacity, numerical analysis**

I. Introduction

With the shortage of traditional energy supplies and the growing environmental problems, there is an urgent need for renewable energy sources to replace traditional fossil energy sources [1]. For renewable energy, wind energy is of great concern to mankind for its cleanliness, safety, efficiency and environmental friendliness [2]. Due to the continuous development of the offshore wind industry, the design of offshore foundation is constantly evolving in terms of capability and design. As coastal wind farms continue to develop into deeper water areas and the capacity of wind turbine generators continue grows, more innovative foundations are needed to satisfy the installation of deep water wind farms, so the hybrid monopile-footing foundation comes into being. The design of the hybrid monopile-footing foundation is based on existing standards for both monopile and gravity foundations, thus accelerating the research into this innovative concept [3–5].

The lateral resistance of hybrid monopile-footing foundation was widely studied by using experiments and numerical simulations in the past few decades. Lehane *et al*. [6, 7] found that the lateral bearing capacity of hybrid monopile-footing foundation was three times higher than that of the original monopile foundations through an experimental centrifuge study. Trojnar [8] carried out full-scale experiments and numerical simulations and showed that the lateral stiffness of the hybrid monopile-footing foundation was increased by 40-70%. Wang *et al.* [3] and Trojnar [8] showed by centrifuge experiments that the failure mechanism was dominated by overturning failure accompanied by slight sliding.

Based on the summary of previous research results, a detailed discussion on hybrid monopile-footing foundations has been carried out, however, due to the lack of comprehensive research on hybrid monopile foundations, so far, the horizontal bearing performance of hybrid monopile-footing foundations in clay soils has not been fully developed. This study therefore focuses on the horizontal bearing characteristics of hybrid monopile-footing foundation in normally consolidated clay soils. Five different soil surface circular footing diameters are considered, and the failure mechanisms of hybrid monopile-footing foundations in different diameters are analysed to explain and predict the overturning resistance of hybrid monopile foundations in clay soils.

II. Numerical Model

In this paper, finite element analysis was carried out using the commercial software ABAQUS version 6.14 and a small strain finite element analysis method was used, considering that the undrained bearing capacity of the hybrid monopile-footing foundation could be fully demonstrated with a small displacement. The hybrid monopile-footing foundation is “wished-in-place” assumption, which means that installation process is ignored, as many have done for skirt foundations [9–12].

A. Hybrid Monopile-footing Model

Fig. 1 shows the geometry of a hybrid monopile-footing

Manuscript received December 7, 2022; revised February 4, 2023; accepted March 17, 2023.

consisting of two basic components, a circular footing placed at the mudline, and a monopile foundation buried in the soil. As shown, the model has a solid monopile with a diameter of 1.1m $(D_p = 1.1m)$ and a pile length of 5.5m $(L_p = 1.1m)$, and a circular foundation with a diameter of 2-10m $(D_w = 2 - 10m)$and a thickness of 0.95m$(t = 0.95m)$ [6–7, 13–14].

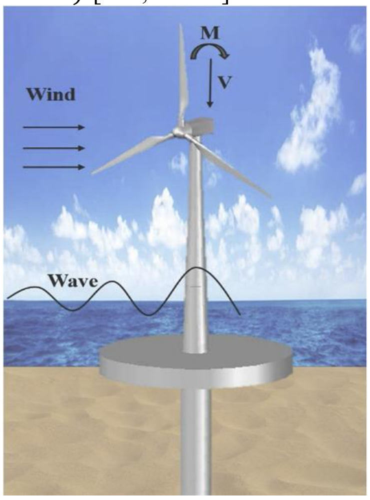

Figure 1. Hybrid monopile-footing foundation.

B. Soil Properties

The soil in this study is a normally consolidated clay, modelled as a linear elastoplastic material, following the Tresca failure criterion (i.e., $\tau_{max} = S_u$) [15]. In order to obtain useful normalized results and to facilitate validation of the existing finite element solutions, the mudline undrained shear strength was idealized to be 5 kPa. The typical small strength at the mudline (0.1 kPa) was not used in this study, as the calculations between them were consistent [15].

The effective unit weight of the soil is $\gamma' = 6kN/m^3$ and Poisson's ratio v is 0.49, which is consistent with the existing marine soft clays [15]. The undrained Young's modulus linearly increasing with depth with constant E_u/S_u =10000, this high rigidity ratio can significantly reduce the cost of calculations as less displacement is required when failure is reached. the high rigidity ratio does not affect the ultimate bearing capacity, comparing the results for E_u/S_u=500 [15].

C. Meshes

In this study, a three-dimensional finite element model is used, and because of the axial symmetry of this model in the vertical direction, a semi-cylindrical model is used for the study, and a typical representative model is shown in Fig. 2. The vertical and horizontal boundaries are set at a distance of $4D_w$ from the footings(D_w is the maximum diameter of a circular footing of 10m) to avoid boundary effects. The top surface of the model is completely free and the bottom surface is fixed in all three coordinate directions. Moreover, the front and sides of the model are constrained for horizontal displacement. All cell meshes of this model are meshed using first order fully integrated hexahedral stress type (C3D8) cell meshes. All models with different D_w are treated using similar meshing principles. The minimum mesh in the model is $0.1D_p$ in the area of gradual refinement near the footing [13–14].

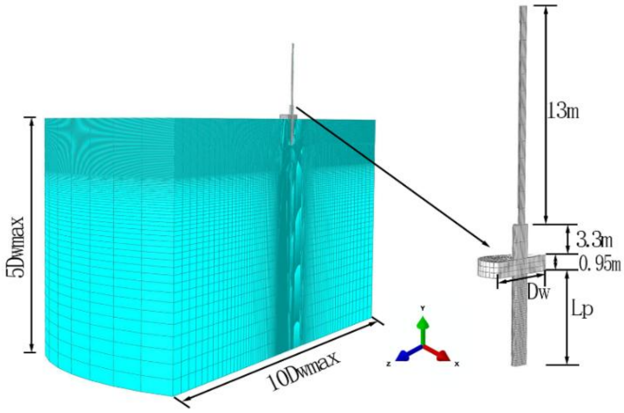

Figure 2. The three-dimensional finite element model.

D. Validation

The sign conventions for loads and displacements adopted in this paper followed the standardized convention suggested by Butterfield *et al.* [4], which had a right-handed system of coordinates and clockwise rotation. Table I presents all the notations adopted and defined in this paper.

There is no exact theoretical solution available for hybrid monopile-footing foundation up to now. However, the accuracy of this study can be verified by comparing the theoretical solution with the known theoretical solution for circular footing and the numerical solution for circular footing of this model, which is listed in Table II.

TABLE I. SUMMARY OF SYMBOLS USED IN THE STUDY [4].

	Vertical	Horizontal	Moment
Load	V	H	M
Ultimate bearing capacity	V_{ult}	H_{ult}	M_{ult}
Bearing capacity factor	$N_{cv} = V_{ult} /AS_u$	$N_{ch} = H_{ult} /AS_u$	$N_{cm} = M_{ult} /ADS_u$
Normalized load	V/V_{ult}	H/H_{ult}	M/M_{ult}
Displacement	v	h	θ

Notification: $A = \frac{1}{4}\pi D^2$ Hybrid monopile circular footing area; S_u; Undrained shear strength at load reference points.

TABLE II. VERIFICATION OF UNIAXIAL BEARING CAPACITY OF CIRCULAR FOOTING.

circular footing	$N_{cv} = V_{ult} /AS_u$	$N_{ch} = H_{ult} /AS_u$	$N_{cm} = M_{ult} /ADS_u$	Authors
Method of characteristics	6.05	—	0.69	Houlsby & Wroth [12,16]
Finite element method	5.91	—	0.69	Gourvenec & Randolph [17,18]
Upper bound results	6.05	—	—	Martin [19]
Finite element method	6.17	1	0.67	Randolph & Puzrin [20]
Finite element method	5.94	1.02	0.71	Fu [21]
Finite element method	6.0260	1.1050	0.7324	This study

III. Results and Discussion

According to the finite element data results, as shown in Fig. 3, it can be found that the lateral displacements to reach the ultimate horizontal bearing capacity of the hybrid monopile-footing foundation with different circular footing diameters are different, the larger the diameter of the circular footing, the larger displacements to reach the ultimate bearing capacity. It can be seen that the ultimate horizontal bearing capacity of the hybrid monopile-footing foundation with a circular footing diameter of 10m is about 6 times the ultimate horizontal bearing capacity of the monopile foundation. It can be seen that the addition of a circular footing at the mudline will greatly increase the horizontal bearing capacity of the monopile.

As shown in Figs. 4 and 5, it can be found that the ultimate horizontal bearing capacity factor of the monopile foundation is the largest, 28.55, and the ultimate horizontal bearing capacity coefficient of the hybrid monopile circular footing foundation with a circular foundation diameter of 10m is the smallest, 2.03. Moreover, with the increasing diameter of the circular footing foundation, the ultimate horizontal bearing capacity factor of the hybrid monopile footing foundation is decreasing. As the diameter of circular footing increases, the horizontal bearing capacity of hybrid monopile-footing foundation gradually transitions from being borne by the monopile to being borne by both of them, and finally to being mainly borne by the circular footing. In this process, the contact section area of foundation keeps increasing, so the bearing capacity factor keeps decreasing.

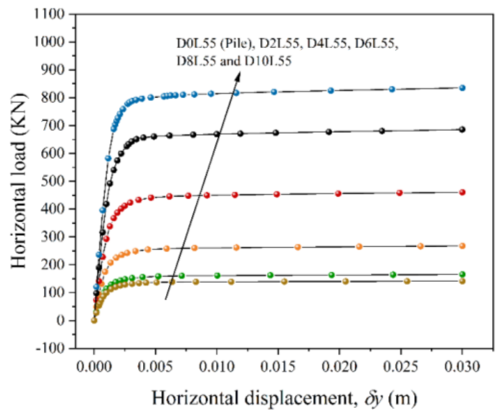

Figure 3. Horizontal bearing capacity curve.

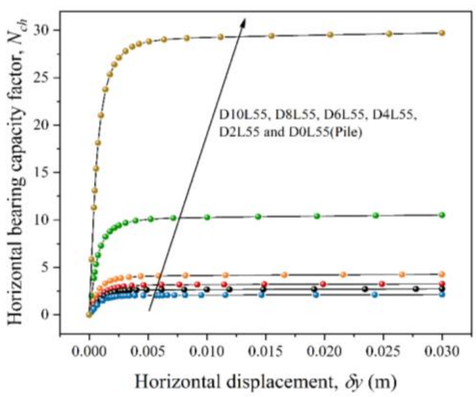

Figure 4. Normalised horizontal load bearing capacity curve.

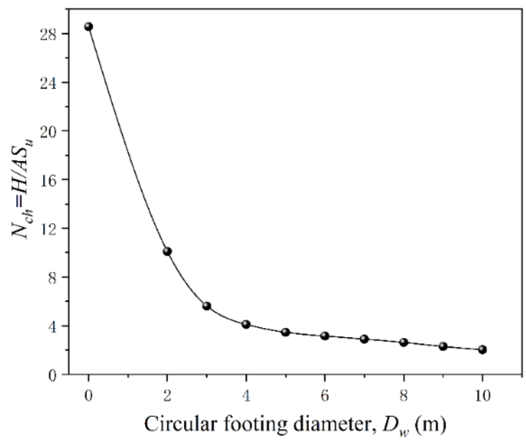

Figure 5. Horizontal load bearing capacity factor curve.

According to Fig. 5, it can be seen that the horizontal load bearing capacity factor curve presents non-linear characteristics, from which we can get the bearing capacity factor and circular footing diameter relationship is not linear. With the increasing diameter of the circular footing, hybrid monopile-footing foundation bearing capacity factor gradually tends to a constant. From the bearing capacity factor curve, it can be analyzed that when the diameter of the circular footing is infinite, the influence of buried piles on the ultimate horizontal bearing capacity of the hybrid monopile-footing foundation can be ignored, and the ultimate horizontal bearing capacity of the hybrid monopile-footing foundation is mainly determined by the circular footing at the mudline.

IV. Conclusion

In this study, the parametric study of the hybrid monopile-footing foundation in cohesive soil has been performed. A series of numerical simulation tests are conducted by considering the effect of circular footing diameters. The influence factors are carefully assessed, and the hybrid monopile foundation is compared with traditional foundations to illustrate the improvement. The analytical methods are proposed to estimate the lateral capacity of the new foundation by using traditional design methods. The following conclusions are drawn from this study:

1) The hybrid monopile foundation demonstrates a larger lateral bearing capacity in cohesive soil compared to the monpile foundation.
2) The lateral capacity increases nonlinearly with the circular footing diameter. this improvement is more pronounced when the circular footing diameter is smaller than 6 m.
3) The failure model of the hybrid monopile-footing foundation includes rotation and translation. The pile and circular footing work systematically to resist the external loadings.

Conflict of Interest

The authors declare no conflict of interest.

Author Contributions

Lei Huang: conceptualization, Investigation, Methodology, Writing original draft, Validation. Jiang Tao Yi: supervision, Resources. Bangju Liu: Resources, Visualization. Xiuzhe Wang: Validation, Resources.

References

[1] R. Mo, R. Cao, M. Liu, and M. Li, "Effect of ground motion directionality on seismic dynamic responses of monopile offshore wind turbines," *Renew. Energy*, vol. 175, pp. 179–199, 2021.

[2] J. Li, X. Wang, and X. Yu, "Use of spatio-temporal calibrated wind shear model to improve accuracy of wind resource assessment," *Appl. Energy*, vol. 213, pp. 469–485, 2018.

[3] X. Wang and J. Li, "Parametric study of hybrid monopile-footing foundation for offshore wind turbines in cohesionless soil," *Ocean Eng.*, vol. 218, 2020, 108172.

[4] R. Butterfield, G. T. Houlsby, G. Gottardi, "Standardized sign conventions and notation for generally loaded foundations," *Géotechnique*, vol. 47, pp. 1051–1054, 1997.

[5] C. Vulpe, S. Gourvenec, and M. Power, "A generalised failure envelope for undrained capacity of circular shallow foundations under general loading," *Géotech. Letter*, vol. 4, pp. 187–96, 2014.

[6] B. Lehane, B. Pedram, J. Doherty, and W. Powrie, "Improved performance of monopiles when combined with footings for tower foundations in sand," *J. Geotech. Geoenviron. Eng.*, vol. 140, no. 7, 2014, 04014027.

[7] B. Lehane, W. Powrie, and J. Doherty, "Centrifuge model tests on piled footings in clay for offshore wind turbines," in *Proc. International Conference in Physical Modelling in Geotechnics*, ICPMG2010. Balkema, Rotterdam, 2010.

[8] K. Trojnar, "Simplified design of new hybrid monopile foundations for offshore wind turbines," *Ocean Eng.*, vol. 219, 2021, 108046.

[9] M. F. Bransdy and M. F. Randolph, "Combined loading of skirted foundations," *Géotechnique*, vol. 48, pp. 637–655, 1998.

[10] D. Fu, C. Gaudin, Y. Tian, B. Bienen, and M. J. Cassidy, "Post-preload undrained uniaxial capacities of skirted circular foundations in clay," *Ocean Eng.* vol. 147, pp. 355–369, 2018.

[11] D. Fu, C. Gaudin, Y. Tian, M. J. Cassidy, and B. Bienen, "Uniaxial capacities of skirted circular foundations in clay," *J. Geotech Geoenviron Eng*, vol. 143, 2017.

[12] G. T. Houlsby and C. P. Wroth, *Calculation of Stresses on Shallow Penetrometers and Footings*, Springer, pp. 107–112, 1984.

[13] K. J. L. Stone, T. A. Newson, M. El Marassi, H. El Naggar, R. N. Taylor, and R. J. Goodey, "An investigation of the use of a bearing plate to enhance the lateral capacity of monopile foundations," *Frontiers in Offshore Geotechnics II. CRC Press*, pp. 641–646, 2010.

[14] K. Stone, T. Newson, and J. Sandon, "An investigation of the performance of a hybrid monopile-footing foundation for offshore structures," *Offshore Site Investigation and Geotechnics, Confronting New Challenges and Sharing Knowledge. Society of Underwater Technology*, 2007.

[15] Y. H. Zhang, B. Bienen, M. J. Cassidy, and S. Gourvenec, "The undrained bearing capacity of a spudcan foundation under combined loading in soft clay," *Mar Struct*, vol. 24, pp. 459–77, 2011.

[16] M. J. Cassidy, C. K. Quah, and K. S. Foo, "Experimental investigation of the reinstallation of spudcan footings close to existing footprints," *J Geotech Geoenviron Eng*, vol. 135, pp. 474–486, 2009.

[17] S. Gourvenec and M. Randolph, "Effect of strength non-homogeneity on the shape of failure envelopes for combined loading of strip and circular foundations on clay," *Géotechnique*, vol. 53, no. 6, pp. 575–586, 2003.

[18] S. Gourvenec and S. Barnett, "Undrained failure envelope for skirted foundations under general loading," *Géotechnique*, vol. 61, pp. 263–270, 2011.

[19] C. M. Martin, "Vertical bearing capacity of skirted circular foundations on Tresca soil," in *Proc. International Conference on Soil Mechanics and Geotechnical Engineering*, 2001, pp. 743-746.

[20] M. F. Randolph and A. M. Puzrin, "Upper bound limit analysis of circular foundations on clay under general loading," *Géotechnique*, vol. 53, no. 9, pp. 785–796, 2003.

[21] D. Fu, "The combined VHM loading capacity of preloaded skirted circular foundations in clay," *School of Civil, Environmental and Mining Engineering*, Univ. of Western Australia, 2017.